Hindered Stepwise Aggregation Model for Molecular Weight Determination of Heavy Petroleum Fractions by Vapor Pressure Osmometry (VPO)

ARTICLE *in* ENERGY & FUELS · MARCH 2013

Impact Factor: 2.79 · DOI: 10.1021/ef302194x

7 AUTHORS, INCLUDING:

Linzhou Zhang
China University of Petroleum
16 PUBLICATIONS **47** CITATIONS
SEE PROFILE

Quan Shi
China University of Petroleum
88 PUBLICATIONS **933** CITATIONS
SEE PROFILE

Chunming Xu
China University of Petroleum
213 PUBLICATIONS **2,642** CITATIONS
SEE PROFILE

Suoqi Zhao
China University of Petroleum
95 PUBLICATIONS **1,077** CITATIONS
SEE PROFILE

energy&fuels

Article

pubs.acs.org/EF

Hindered Stepwise Aggregation Model for Molecular Weight Determination of Heavy Petroleum Fractions by Vapor Pressure Osmometry (VPO)

Linzhou Zhang,[†] Quan Shi,*[,†] Changsen Zhao,[†] Na Zhang,[†] Keng H. Chung,[‡] Chunming Xu,[†] and Suoqi Zhao*[,†]

[†]State Key Laboratory of Heavy Oil Processing, China University of Petroleum, Beijing 102249, People's Republic of China

[‡]Well Resources, Incorporated, 3919-149A Street, Edmonton, Alberta T6R 1J8, Canada

Supporting Information

ABSTRACT: Venezuela Orinoco heavy crude oil was fractionated into diesel, vacuum gas oil (VGO), vacuum residue (VR), and asphaltene fractions, which were subjected to molecular weight (MW) measurement by vapor pressure osmometry (VPO). The VPO is known to overestimate the average molecular weight (MW) of heavy hydrocarbons, because of molecular aggregation. This paper proposes a hindered stepwise aggregation (HSA) model to simulate the molecular aggregation and used the model to estimate the true MW of heavy petroleum fractions. A data regression procedure was developed to determine the model parameters, aggregation equilibrium constant, and aggregate distribution, using a fast simulated annealing (FSA) algorithm based on the VPO data. This data analysis method is self-tuned to fit the VPO data to the HSA models of various petroleum fractions using the optimized solution of the FSA algorithm. The results showed that the VPO data of heavy petroleum fractions at various solution concentrations were in good agreement with those predicted by the HSA model. The aggregation equilibrium constant and aggregate distribution data obtained from the HSA model suggested that various degrees of molecular aggregation occur in heavy petroleum fractions. The molecules of diesel and VGO were monomers, regardless of the solution concentration. The molecules of VR formed dimer aggregates at high solution concentrations; the number of dimer aggregates exceeded that of monomers as the solution concentration increased. The molecules of asphaltenes were polymer aggregates. The size of asphaltene polymer aggregates increased significantly with the solution concentration. The MW of asphaltenes determined by the HSA model was much lower than that by the conventional linear regression method.

INTRODUCTION

Petroleum is an extremely complex hydrocarbon mixture. Over the years, tremendous efforts have been devoted to improve petroleum processing systems and clean fuel use. Among the chemical and physical properties of petroleum-derived streams, molecular weight (MW) is commonly used to define and correlate petroleum systems.[1−3] The MW of petroleum feedstock is also the key design parameter used to develop catalysts.[4]

There are several methods used for determining the MW of petroleum systems, including vapor pressure osmometry (VPO), gel permeation chromatography (GPC), and mass spectrometry (MS).[5−11] Among them, VPO is the most commonly used technique, because of its simplicity and low costs. VPO provides the average MW of a bulk sample based on thermodynamic equilibrium, which minimizes or eliminates the influence of molecular diversity created by varying GPC calibration curves and MS ionization efficiency.[10,12−14] However, VPO is an inadequate technique for heavy petroleum fractions, especially asphaltenes. The asphaltene molecules are large aromatic rings with many heteroatoms, which exhibit strong molecular association.[15−17] This leads to the formation of aggregates that cause severe deviations in VPO MW measurements.[15,18,19] The VPO MW of the heavy petroleum fraction is known to increase nonlinearly with the solution concentration. Conventional linear regression analysis is inadequate to fit the VPO data for strong molecular association systems.[18] Moreover, the VPO MW is dependent upon the solvent type and operating temperature.[20] For strong molecular association systems, the formation of aggregates occurs at relatively low solution concentrations (10^{-4} mass fraction for asphaltenes),[15] which are beyond the operating window of VPO analysis.

Molecular aggregation in heavy petroleum fractions not only affects MW measurements[21−24] but also contributes to the discrepancies in the chemistry of asphaltenes found in the literature.[9,25,26] Hence, the development of a more accurate MW measurement technique and a better understanding of molecular aggregation in heavy petroleum systems[22,27−31] are important to petroleum science research. Asphaltene flocculation causes pipeline plugging and fouling. This process is attributed to molecular aggregation.[32] Molecular aggregation influences the transport phenomena of petroleum species in refinery processes. For some supermolecular systems, the size of the aggregate can be considered as associated bonds.[33,34] However, there is currently no effective method to determine the aggregate distribution of petroleum because of the complex intermolecular association in the substance.[35] Molecular

Received: January 2, 2013
Revised: February 24, 2013
Published: February 26, 2013

dx.doi.org/10.1021/ef302194x | Energy Fuels 2013, 27, 1331−1336

aggregation also occurs in other complex heavy hydrocarbon systems, such as with coal-derived materials.[36,37]

Attempts have been made previously to model the molecular aggregation to correct VPO MW data for heavy petroleum fractions. Yarranton et al.[38] fitted the asphaltene VPO data to a nonlinear function, which lacked physical meaning.[38] Then, they proposed a self-association model for asphaltene aggregates analogous to linear polymerization.[39] The model defined the asphaltene molecules as "propagators" and "terminators" by their functionalities in molecular aggregation and assumed a constant molecular association. The effects of resins and asphaltenes on molecular aggregation were investigated using the attenuated association constant.[40] Because molecular aggregation is a highly coupled nonlinear system, the mathematical expression of the molecular aggregation model is an implicit function. The challenge is to develop an algorithm to determine the parameters of an implicit mathematical function using the VPO MW data.

In this paper, the hindered stepwise aggregation (HSA) model was used to simulate the aggregation of hydrocarbon molecules and determine the true MWs of heavy petroleum fractions from VPO data. A self-tuned data analysis method was developed to fit the VPO data to the HSA model and iterated by itself to determine the parameters of the aggregation model.

THEORY

Ideal and Aggregation System. Figure 1 shows the dispersed molecules in an ideal and aggregation system and the

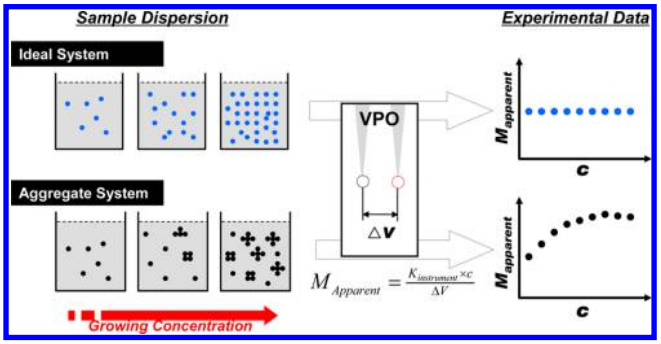

Figure 1. Sample dispersion in the ideal and aggregate systems and their corresponding VPO data plots. The apparent MW ($M_{apparent}$) of the bulk sample is calculated from the voltage response of the detect poles. For an ideal system, the apparent MW is independent of the concentration. For a high aggregate system, the apparent MW grows nonlinearly with the concentration, indicating that application of linear regression is not appropriate.

corresponding VPO MW as a function of the solution concentration. In an ideal dispersed system, there are no molecular interactions and the molecules remain dispersed, regardless of the solution concentration. The apparent MW remains constant with the solution concentration. In theory, only one VPO MW measurement is needed for an ideal system, which is the basis for the ASTM D-2503 method. However, because of the experimental error, multiple VPO MW measurements (generally four data points) are recommended and the apparent MW is obtained by linear regression of these measurements. In the case where molecular interactions are relatively low, the error in the linear regression is low and commonly ignored.

In a solution with strong interaction forces among the molecules, such as hydrogen bonds, $\pi-\pi$ stacking, and metal coordination,[41] the molecules form aggregates. The apparent MW increases as the solution concentration increases. Hence, large deviations are can occur from linear regression of VPO data. Previous VPO analysis on the asphaltenes and hexabenzocoronene showed a nonlinear dependency of the apparent MW to the solution concentration.[42]

HSA Model. Figure 2 shows the schematic diagram of the stepwise aggregation of molecules. The HSA model assumes

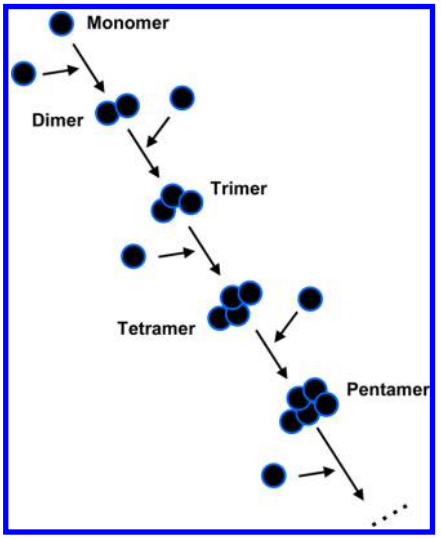

Figure 2. Stepwise growth of the aggregate in the solvent. The larger aggregate is formed by effective collision between the smaller aggregate and monomer.

that the size of aggregates increases as a result of the effective interaction/collision among monomers. The formation of large aggregates results from sequential collisions of monomers with smaller aggregates. The large aggregates do not originate from the collisions of monomers, and the aggregate−aggregate collisions are ignored.

Each sequential aggregation is assigned a specific association constant, K. A description of K values assigned for various types of aggregation has been provided elsewhere.[43] The probability of aggregate formation for large aggregates diminishes, because of increased steric hindrance and decreased interactive sites. Large aggregates also have low entropies, which are detrimental to the growth of larger aggregates. Therefore, it is reasonable to have a diminished K value as the size of the aggregate increases. In this study, the diminished K_{i+1} value for each subsequent aggregation i can be obtained by multiplying K by a hindrance factor, H, as shown in eq 1

$$K_{i+1} = K_i H \tag{1}$$

where the value of H is assumed to be constant for each step. A hindrance factor was also used by Yarranton et al.[40] Scheme 1 (see the Supporting Information) illustrates the mathematical representations of the HSA model. If $H = 1$, the HSA model is an equal stepwise aggregate K model. If $H = 0$, only the formation of dimer aggregates will occur and the HSA model is applicable to systems in which the molecules have only one active site.

From Scheme 1, the apparent MW, $MW_{apparent}$, and the mass concentration of the system, c, can be expressed as follows:

dx.doi.org/10.1021/ef302194x | Energy Fuels 2013, 27, 1331−1336

Scheme 1

Reaction Expression	Aggregator Concentration	Associate Constant
$A_1 + A_1 \xrightarrow{K_1} A_2$	$C(A_2) = K_1 C^2(A_1)$	
$A_2 + A_1 \xrightarrow{K_2} A_3$	$C(A_3) = K_2 C(A_2) C(A_1)$	$K_2 = K_1 \times H$
$A_3 + A_1 \xrightarrow{K_3} A_4$	$C(A_4) = K_3 C(A_3) C(A_1)$	$K_3 = K_1 \times H^2$
.....	.....	.....
$A_{n-1} + A_1 \xrightarrow{K_{n-1}} A_n$	$C(A_n) = K_{n-1} C(A_{n-1}) C(A_1)$	$K_{n-1} = K_1 \times H^{n-2}$

$$M_{\text{apparent}} = \frac{M_N \sum_1^n [iC(A_1)^i K_1^{i-1} H^{(i-2)(i-1)/2}]}{\sum_1^n [C(A_1)^i K_1^{i-1} H^{(i-2)(i-1)/2}]} \quad (2a)$$

$$c = M_N \sum_1^n [iC(A_1)^i K_1^{i-1} H^{(i-2)(i-1)/2}] \quad (2b)$$

where M_N is the MW of monomers, $C(A_1)$ is the molar concentration of monomers in the system, K_1 is the steady-state association constant of the first aggregation step, and n is the maximum number of aggregates in the system.

Experimentally, the $MW_{apparent}$ is the measured VPO MW, and c can be calculated from the molecular mass and volume of the sample in the dilute solvent system.

Computation Algorithm. The computation algorithm for the HSA model is shown in Figure 3. The experimental data,

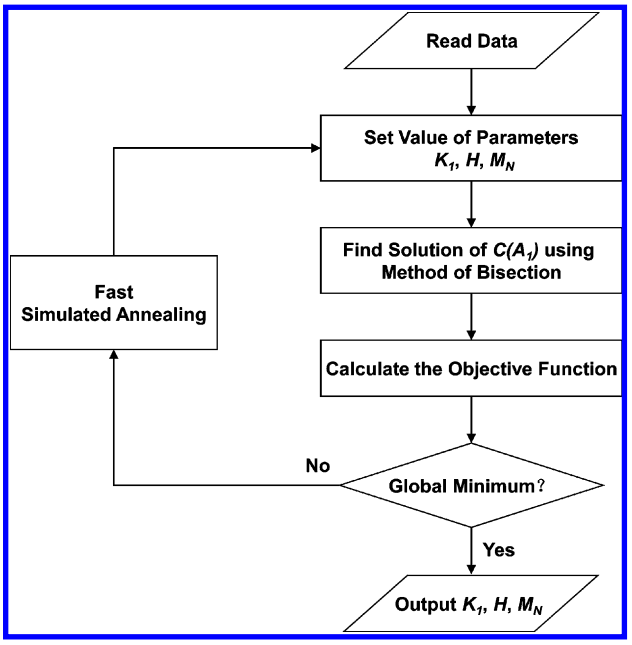

Figure 3. Schematic of the model-solving procedure for the HSA model.

$MW_{apparent}$ and c, were input into the computer program, along with the initial estimated parameters, MW_N, K_1, and H. The objective function is defined as the variation between the predicted and measured data. The concentration of monomers $[C(A_1)]$ was calculated from eq 2b using the method of bisection to determine the value of the objective function. The n value was set to 100; aggregates with more than 100 monomers were not considered.

The final optimized solution was determined using a fast simulated annealing (FSA) algorithm. The simulated annealing (SA) algorithm is effective in solving the NP-complete problems.[44] However, the classic SA algorithm is time-consuming. To speed up the computation, Szu et al.[45] proposed the FSA algorithm using Cauchy distribution to generate perturbation on the solution and modified the annealing procedure accordingly. The Cauchy distribution is a fat-tail distribution, which allows for the FSA to vary from the local minimum even at very low annealing temperatures and increases the possibility of reading a global minimum. The computation algorithm for FSA is shown in Figure 4. The

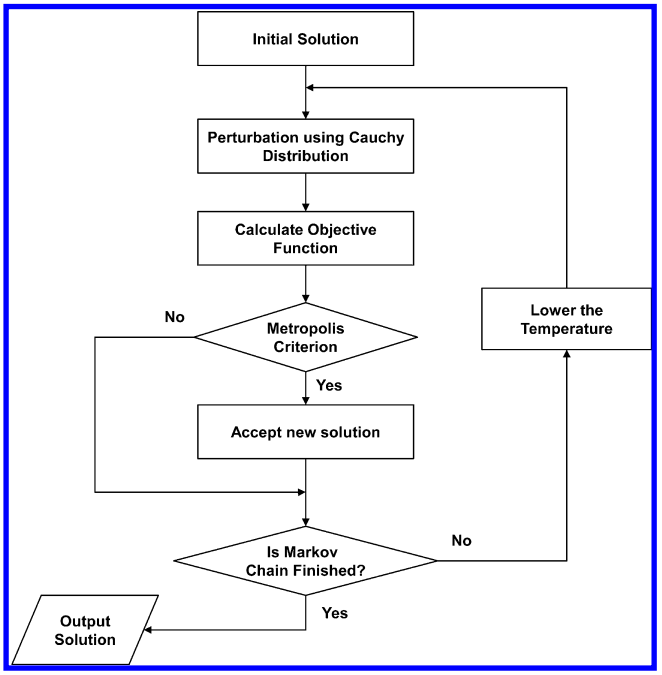

Figure 4. Schematic of the FSA algorithm.

parameters of the HSA model were obtained using the FSA algorithm, in which the values of parameters yielded the global minimum of the objective function. The pseudo-code for the program is available in the Supporting Information.

The FSA computation procedure was as follows. The values of parameters were varied randomly, which yielded an objective function value. After the iteration, a global minimum solution of the objective function was determined and the parameters that best fitted the experimental data were obtained. During iterations, the MW varied from 50% of the apparent MW at the lowest solution concentration to 100% of the apparent MW at the highest solution concentration. Because the FSA algorithm is a probabilistic metaheuristic search method, the results using different searches would vary slightly. In this work, MATLAB (Mathworks, Natick, MA) was used for numerical computations.

EXPERIMENTAL SECTION

Materials. Venezuela Orinoco heavy crude oil was distilled using a laboratory distiller into three fractions: diesel (180−350 °C), vacuum gas oil (VGO, 350−500 °C), and vacuum residue (VR, 500 °C+). Asphatenes was obtained from the VR by precipitation using *n*-pentane (*n*-C_5) as the solvent, according to the ASDM 2007-80 standard.

Instrumentation. The MW measurements were performed using a K-7000 vapor pressure osmometer (Knauer, Germany) with toluene as the solvent. The analytical reagent (AR)-grade toluene was distillated twice to remove contaminants prior to use. Sucrose octaacetate (679

dx.doi.org/10.1021/ef302194x | *Energy Fuels* 2013, 27, 1331−1336

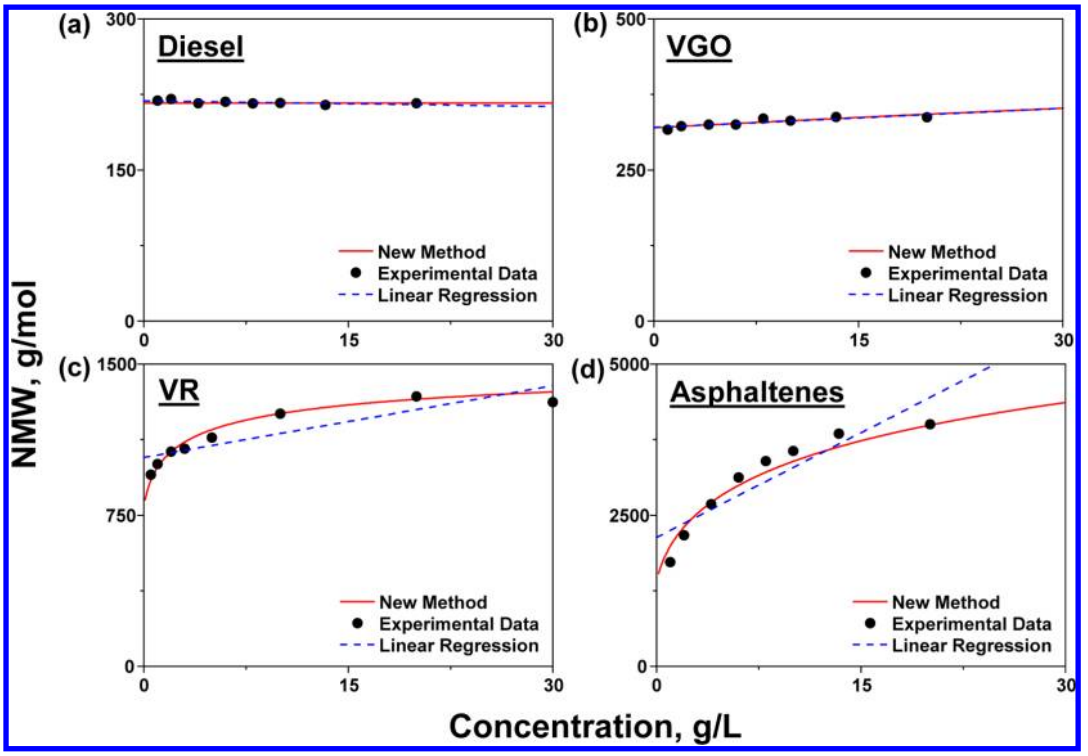

Figure 5. Experiment data and prediction from the new analysis method and traditional linear regression for four petroleum fractions. The HSA model fitted well to all of the fractions. On the contrary, linear regression only shows good agreement with the experiment for low-aggregate diesel and VGO fractions. For high-aggregate VR and asphaltene fractions, obvious derivations were observed.

g/mol) was used to calibrate the VPO instrument. A diluted oil sample was prepared by mixing a predetermined amount of oil sample with 10 mL of toluene. For each oil fraction, eight diluted oil samples were prepared in concentrations varying from 0.5 to 30 g/L. The diluted oil sample was introduced to the VPO instrument, which was maintained at 60 °C for 2 h. The drops at the VPO detect poles were inspected and manually controlled to a similar size to minimize the deviation of drop shapes.[46] The original voltage responses (ΔV) were recorded and converted into apparent MW using an Excel spreadsheet (Microsoft, Redmond, WA). For each solution concentration, the VPO MW measurement was repeated 3 or 4 times, and the mean VPO MW value was determined. The VPO MW data at various concentrations were input to the MATLAB software and used to calculate the parameters of the HSA model.

RESULTS AND DISCUSSION

HSA Model versus Linear Regression. Figure 5 shows the VPO MW as a function of the solution concentration for diesel, VGO, VR, and asphaltene fractions. As shown in panels a and b of Figure 5, the VPO MWs of diesel and VGO were relatively constant or slightly dependent upon the solution concentration, indicating highly non-interacting molecular systems. The predictions from the linear regression method and HSA model were in good agreement with the VPO MW data.

Panels c and d of Figure 5 show the VPO MW as a function of the solution concentration for VR and asphaltene, respectively. MW increased dramatically at low solution concentrations (up to 10 g/L) and then remained constant at high concentrations, indicating high interacting molecular systems. As expected, the predictions from the linear regression method exhibited high deviations from the nonlinear VPO MW data, especially at zero solution concentration. The predictions from the HSA method were in good agreement with the VPO MW data.

In summary, the data in Figure 5 show that the predictions using the linear regression method are adequate only for light petroleum fractions, while those using the HSA model are adequate for all of the petroleum fractions.

MW and Associate Constant. Table 1 summarizes the predicted MWs of diesel, VGO, VR, and asphaltene determined by the linear regression and HSA model and the corresponding average absolute deviations (AADs) between the measured and predicted MWs. Also shown in Table 1 are the values of K_1 and H (parameters of the HSA model) that best fit the VPO MW data for the four petroleum fractions. The MWs and AADs of diesel and VGO determined by the linear regression and HSA model were similar. For the VR and asphaltene, the MWs determined by the HSA model were much lower than those from the linear regression. The MW of asphaltenes was 1404.2

Table 1. Parameters and AAD of the New Method and Traditional Linear Regression for Petroleum Fractions

	HSA				linear regression	
fraction	M_N (g/mol)	K_1 (L/mol)	H	AAD (%)	M_N (g/mol)	AAD (%)
diesel	216.3	0.0	0.6[a]	0.6	218.5	0.5
VGO	319.7	1.2	0.9[a]	0.8	320.2	0.8
VR	788.3	441.4	0.0	2.1	1036.5	4.7
asphaltene	1404.8	975.6	0.8	5.4	2131.3	10.7

[a]The H value was not convergence and stable after iterations in diesel and VGO, because the hindrance factor does not form measurable impact on the system when the associate constant (K_1) is ultralow or even zero. The value here is the final output by software but without any physical meaning.

dx.doi.org/10.1021/ef302194x | Energy Fuels 2013, 27, 1331−1336

g/mol using the HSA model and 2131.3 g/mol using the linear regression. The values of AAD of the HSA model were also lower than those of the linear regression.

For the HSA model, the parameter K_1 denotes the associate constant of dimer formation, which is also the initial aggregation process. The K_1 values for diesel and VGO were low at 0.0 and 1.2, respectively, indicating that they are ideal solution systems. The H values for diesel and VGO generated by the HSA model were physically insignificant for ideal solution systems without aggregation. The K_1 and H values of VR were lower than those of asphaltenes, indicating that asphaltenes have a higher tendency to form aggregates but have a slower growth rate of the aggregate size.

From the HSA model and VPO MWs of VR and asphaltene as a function of the solution concentrations, the aggregation characteristics of asphaltenes can be deduced. When asphaltenes are in their native state and stably suspended in less polar fractions of VR, i.e., aromatics and resins, the asphaltene molecules have low probability to have effective collisions, resulting in increased aggregate size. Therefore, by the complementary use of the HSA model, the VPO analysis is not only capable of determining the MW of heavy hydrocarbons, but is also a useful analysis tool for investigating the aggregation characteristics of a high molecular interaction system.

Aggregate Size Distribution. From the HSA model, the aggregate size distribution of molecules in solution can be determined. Figure 6 shows the aggregate size distributions of the four petroleum fractions at various solution concentrations (1, 10, and 20 g/L). Diesel existed as monomers, regardless of solution concentrations. VGO was primarily monomers with relatively small numbers of dimers forming as the solution concentration increased. For VR and asphaltene, monomers were dominant at the low solution concentration (1 g/L). For VR, as the concentration increased, the number of dimers exceeded that of monomers. Because of the hindrance of aggregate size growth, no polymers were found. For asphaltenes, various size aggregates were found at the low solution concentration. As the solution concentration increased, the fraction of large aggregates increased.

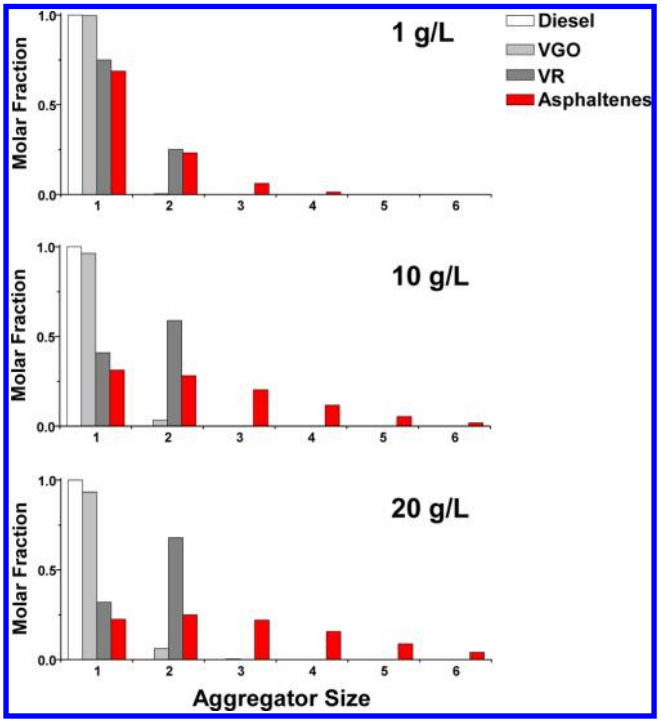

Figure 6. Aggregate size distribution for petroleum fractions in different concentrations calculated from the HSA model. In both high and low concentrations, the monomer dominates the diesel and VGO toluene solutions. VR has very high aggregate hindrance, in which the dimer is the largest aggregate. Even in a very low concentration (1 g/L), the multimers form in asphaltene toluene solution. As the concentration grows, the molar fractions of multimers exceed the content of the monomer.

CONCLUSION

The HSA molecular aggregation model was developed and used to correct the VPO MW data for heavy petroleum fractions. The results showed that the VPO data of heavy petroleum fractions at various solution concentrations were in good agreement with those predicted by the HSA model. By comparison, the linear regression method used in conventional VPO data treatment showed that the linear regression method overestimated the MW of heavy petroleum fractions at low solution concentrations. The aggregation equilibrium constant and aggregate distribution data obtained from the HSA model suggested that various degrees of molecular aggregation occur in heavy petroleum fractions. The molecules of diesel and VGO were monomers, regardless of the solution concentration. The molecules of VR formed dimer aggregates at high solution concentrations; the number of dimer aggregates exceeded that of monomers as the solution concentration increased. The molecules of asphaltenes were polymer aggregates. The size of asphaltene polymer aggregates increased significantly with the solution concentration. The MW of asphaltenes determined by the HSA model was much lower than that by the linear regression method.

ASSOCIATED CONTENT

Supporting Information

Pseudo-code for the model-solving program. This material is available free of charge via the Internet at http://pubs.acs.org.

AUTHOR INFORMATION

Corresponding Author

*Telephone: +86-10-8973-3738 (Q.S.); +86-10-8973-9015 (S.Z.). E-mail: sq@cup.edu.cn (Q.S.); sqzhao@cup.edu.cn (S.Z.).

Notes

The authors declare no competing financial interest.

ACKNOWLEDGMENTS

The authors thank Dr. Zhentao Chen for helpful discussion on the molecular size and aggregation of petroleum molecules, Xuxia Liu for assistance in VPO analyses, and Yang Liu for providing the asphaltene samples. This work was supported by the National Basic Research Program of China (2010CB226901) and the National Natural Science Foundation of China (NSFC) (U1162204 and 21176254).

REFERENCES

(1) Riazi, M. *Characterization and Properties of Petroleum Fractions*; ASTM International: West Conshohocken, PA, 2005.

(2) Speight, J. G. *The Chemistry and Technology of Petroleum*; CRC Press (Taylor and Francis Group): Boca Raton, FL, 2007.

(3) Shi, T.-P.; Xu, Z.-M.; Cheng, M.; Hu, Y.-X.; Wang, R.-A. *Energy Fuels* **1999**, *13* (4), 871−876.
(4) Chen, Z.; Xu, C.; Gao, J.; Zhao, S.; Xu, Z. *AIChE J.* **2010**, *56* (8), 2030−2038.
(5) Roussis, S. G.; Proulx, R. *Anal. Chem.* **2002**, *74* (6), 1408−1414.
(6) Becker, C.; Qian, K.; Russell, D. H. *Anal. Chem.* **2008**, *80* (22), 8592−8597.
(7) Mori, S. *Anal. Chem.* **1981**, *53* (12), 1813−1818.
(8) Schriemer, D. C.; Li, L. *Anal. Chem.* **1996**, *68* (17), 2721−2725.
(9) Herod, A. A.; Bartle, K. D.; Kandiyoti, R. *Energy Fuels* **2007**, *21* (4), 2176−2203.
(10) Qian, K.; Edwards, K. E.; Siskin, M.; Olmstead, W. N.; Mennito, A. S.; Dechert, G. J.; Hoosain, N. E. *Energy Fuels* **2007**, *21* (2), 1042−1047.
(11) Herod, A. A.; Bartle, K. D.; Morgan, T. J.; Kandiyoti, R. *Chem. Rev.* **2012**, *112* (7), 3892−3923.
(12) Amad, M. A. H.; Cech, N. B.; Jackson, G. S.; Enke, C. G. *J. Mass Spectrom.* **2000**, *35* (7), 784−789.
(13) Cech, N. B.; Enke, C. G. *Mass Spectrom. Rev.* **2001**, *20* (6), 362−387.
(14) Qian, K.; Edwards, K. E.; Diehl, J. H.; Green, L. A. *Energy Fuels* **2004**, *18* (6), 1784−1791.
(15) Mullins, O. C. *Energy Fuels* **2010**, *24* (4), 2179−2207.
(16) Mullins, O. C.; Sabbah, H.; Eyssautier, J.; Pomerantz, A. E.; Barré, L.; Andrews, A. B.; Ruiz-Morales, Y.; Mostowfi, F.; McFarlane, R.; Goual, L.; Lepkowicz, R.; Cooper, T.; Orbulescu, J.; Leblanc, R. M.; Edwards, J.; Zare, R. N. *Energy Fuels* **2012**, *26* (7), 3986−4003.
(17) Gray, M. R.; Tykwinski, R. R.; Stryker, J. M.; Tan, X. *Energy Fuels* **2011**, *25* (7), 3125−3134.
(18) Rakotondradany, F.; Fenniri, H.; Rahimi, P.; Gawrys, K. L.; Kilpatrick, P. K.; Gray, M. R. *Energy Fuels* **2006**, *20* (6), 2439−2447.
(19) Acevedo, S. C.; Guzman, K.; Ocanto, O. *Energy Fuels* **2010**, *24* (3), 1809−1812.
(20) Moschopedis, S. E.; Fryer, J. F.; Speight, J. G. *Fuel* **1976**, *55* (3), 227−232.
(21) Pomerantz, A. E.; Hammond, M. R.; Morrow, A. L.; Mullins, O. C.; Zare, R. N. *J. Am. Chem. Soc.* **2008**, *130* (23), 7216−7217.
(22) Spiecker, P. M.; Gawrys, K. L.; Kilpatrick, P. K. *J. Colloid Interface Sci.* **2003**, *267* (1), 178−193.
(23) Smith, D. F.; Schaub, T. M.; Rahimi, P.; Teclemariam, A.; Rodgers, R. P.; Marshall, A. G. *Energy Fuels* **2007**, *21* (3), 1309−1316.
(24) Behrouzi, M.; Luckham, P. F. *Energy Fuels* **2008**, *22* (3), 1792−1798.
(25) Herod, A. A.; Bartle, K. D.; Kandiyoti, R. *Energy Fuels* **2008**, *22* (6), 4312−4317.
(26) Mullins, O. C.; Martnez-Haya, B.; Marshall, A. G. *Energy Fuels* **2008**, *22* (3), 1765−1773.
(27) Liu, Y. C.; Sheu, E. Y.; Chen, S. H.; Storm, D. A. *Fuel* **1995**, *74* (9), 1352−1356.
(28) Dabir, B.; Nematy, M.; Mehrabi, A. R.; Rassamdana, H.; Sahimi, M. *Fuel* **1996**, *75* (14), 1633−1645.
(29) Rassamdana, H.; Dabir, B.; Nematy, M.; Farhani, M.; Sahimi, M. *AIChE J.* **1996**, *42* (1), 10−22.
(30) Rassamdana, H.; Sahimi, M. *AIChE J.* **1996**, *42* (12), 3318−3332.
(31) Mozaffarian, M.; Dabir, B.; Sohrabi, M.; Rassamdana, H.; Sahimi, M. *Fuel* **1997**, *76* (14−15), 1479−1490.
(32) Mullins, O. C.; Hammami, A.; Marshall, A. G. *Asphaltenes, Heavy Oils, and Petroleomics*; Springer: New York, 2007.
(33) Watson, M. D.; Fechtenkotter, A.; Mullen, K. *Chem. Rev.* **2001**, *101* (5), 1267−1300.
(34) Micali, N.; Monsu' Scolaro, L.; Romeo, A.; Mallamace, F. *Phys. A* **1998**, *249* (1−4), 501−510.
(35) da Costa, L. M.; Stoyanov, S. R.; Gusarov, S.; Tan, X.; Gray, M. R.; Stryker, J. M.; Tykwinski, R. R.; de M. Carneiro, J. W.; Seidl, P. R.; Kovalenko, A. *Energy Fuels* **2012**, *26* (5), 2727−2735.
(36) Ghosh, A. K.; Srivastava, S. K.; Bagchi, S. *Fuel* **2007**, *86* (16), 2528−2534.
(37) Wang, Z.; Li, L.; Shui, H.; Wang, Z.; Cui, X.; Ren, S.; Lei, Z.; Kang, S. *Fuel* **2011**, *90* (1), 305−311.
(38) Yarranton, H. W.; Alboudwarej, H.; Jakher, R. *Ind. Eng. Chem. Res.* **2000**, *39* (8), 2916−2924.
(39) Agrawala, M.; Yarranton, H. W. *Ind. Eng. Chem. Res.* **2001**, *40* (21), 4664−4672.
(40) Yarranton, H. W.; Fox, W. A.; Svrcek, W. Y. *Can. J. Chem. Eng.* **2007**, *85* (5), 635−642.
(41) De Greef, T. F. A.; Smulders, M. M. J.; Wolffs, M.; Schenning, A. P. H. J.; Sijbesma, R. P.; Meijer, E. W. *Chem. Rev.* **2009**, *109* (11), 5687−5754.
(42) Rakotondradany, F.; Fenniri, H.; Rahimi, P.; Gawrys, K. L.; Kilpatrick, P. K.; Gray, M. R. *Energy Fuels* **2006**, *20* (6), 2439−2447.
(43) Martin, R. B. *Chem. Rev.* **1996**, *96* (8), 3043−3064.
(44) Kirkpatrick, S.; Gelatt, C. D.; Vecchi, M. P. *Science* **1983**, *220* (4598), 671−680.
(45) Szu, H.; Hartley, R. *Phys. Lett. A* **1987**, *122* (3−4), 157−162.
(46) Meeks, A. C.; Goldfarb, I. J. *Anal. Chem.* **1967**, *39* (8), 908−911.